Indian J. Phys. **44**, 172–187, (1970)

Effects of external circuit on heat transfer in MHD channel flow

By V. M. Soundalgekar, *Department of Mathematics*,
B. V. Rao. *Department of Electrical Engineering*,
Indian Institute of Technology, Bombay (76),
D. D. Haldavnekar, *Univ. Dept. of Chemical Technology, Bombay*-19
R. S. Iyer, *Engineer, Larsen and Toubro, Bombay*

(*Received* 20 *December* 1969, *revised* 19 *June* 1970)

An analysis of heat transfer in fully developed mhd channel flow has been presented. Closed form solutions in case of (i) two plates at constant temperatures, and (ii) linear variation of temperature along the plates, are derived for temperature, Nusselt number, mean-mixed temperature and the difference between the wall temperature and the mean fluid temperature. Numerical values of the Nusselt number and mean-mixed temperature are entered in tables, whereas, others are shown graphically. The effects of different parameters in different types of channel flows have been discussed.

Nomenclature

A	Temperature gradient	S	A non-dimensional number
B_0	Magnetic field (applied)	S_1	A non-dimensional number
C_p	Specific heat at constant pressure	T	Temperature
G	Temperature	T_{lm}	Mean mixed temperature
G^*	Non-dimensional temperature	u	Velocity in x-direction
I	Total current		Non-dimensional velocity
I^*	Non-dimensional total current		Average velocity
J^*	Non-dimensional current density	V_g	External generator voltage
J_z	Current density	V_g^*	Non-dimensional external generator voltage
K	Thermal conductivity		
Nu	Nusselt number	x	Co-ordinate along the plates
M	Hartmann number	$2y_0$	Separation between two plates
P	Pressure	y	co-ordinate normal to the x-axis
Pr	Prandtl number	z	Normal to xy-axes
q	Heat flux at the plates	ρ	density
Q	Non-dimensional heat flux	θ	Non-dimensional temperature
R	Resistance	σ	Electrical conductivity
Re	Reynolds number	η	Non-dimensional transverse axis
R^*	Non-dimensional resistance	μ	Viscosity

1. Introduction

Hartmann (1937) and Hartmann & Lazarus (1937) studied the mhd channel flow under a transverse magnetic field. From technological point of view, the heat transfer aspect of such flow is important. Sutton & Sherman (1965) studied this aspect under the action of the loading parameter, thus distinguishing the channel as an mhd generator, accelerator or flowmeter. The heat transfer has also been studied by Siegel (1958) in open circuit mhd channel flow between non-conducting plates, whereas, between conducting plates, it was discussed independently by Alpher (1961) and Yen (1963). Recently, Soundalgekar (1969) studied the heat transfer aspect of mhd channel flow between conducting walls and under crossed-fields. But to understand the working of the channel in the most general way, the external circuit must also be considered. Such an analysis was recently presented by Hughes & Young (1966) who considered the circuit consisting of a resistance and a generator, and thus characterised the mhd channel flow in different ways. The heat transfer aspect of such a system has not been considered as yet. This provides the motivation to undertake the present study.

In section 2, while presenting the mathematical analysis, two cases are considered :—(1) two plates at different temperatures and (2) linear variation of the temperature along the plates in the direction of the flow. Following Hughes & Young (1966) we have derived the closed form solutions for the velocity, current density and total current. Using these expressions, closed form solutions for temperature, Nusselt number and the mean mixed temperature are derived in case (1) whereas, in case (2) closed form solutions for the temperature, Nusselt number and the differnce between wall temperature and mean temperature of the fluid are derived. Numerical values of Nusselt number in cases 1 and 2 and for the mean mixed temperature in case 1 are entered in tables 1 to 3, whereas, other physical quantities are shown on graphs

In section 3, conclusions are set out.

2. Mathematical Analysis

Here the x-axis is taken along the centre-line of the channel in the direction of the flow and y-axis is chosen normal to the x-axis. The magnetic field is assumed to be applied parallel to the y-axis. The external circuit is given in figure 1a.

Under these conditions, following Hughes & Young (1966), the expressions for the velocity and the current density for fully developed flow can be derived as follows :

$$u^* = \frac{\coth M}{M} \cdot \frac{1+R^*+MV_g^*}{R^*+M\coth M} \cdot \frac{1-\cosh M\eta}{\cosh M} \qquad \ldots (1)$$

$$J^* = \frac{(I^*-1)M}{\sinh M} \cosh M\eta + 1, \qquad \ldots (2)$$

$$I^* = \frac{V_0^* - \left(\frac{1}{M} - \coth M\right)}{R^* + M \coth M}, \qquad \ldots (2a)$$

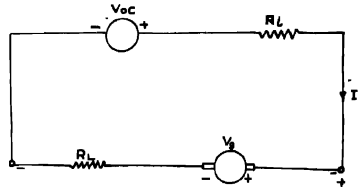

Figure 1a The complete electrical circuit.

where the physical quantities are defined in non-dimensional form as follows :

$$\left.\begin{aligned} u^* &= \frac{u}{(y_0^2/\mu)\left(-\frac{\partial p}{\partial x}\right)}\ ;\ \eta = \frac{y}{y_0};\ R^* = \frac{R}{(Z_0/2\sigma x_0 y_0)}\ ; \\ V_0^* &= \frac{V_0}{(2y_0 z_0/\sqrt{\sigma\mu})\left(-\frac{\partial p}{\partial x}\right)}\ ;\ M = y_0 B_0 \sqrt{\sigma/\mu}\ ; \\ I^* &= \frac{I}{\left[4x_0 y_0^2 \sqrt{\frac{\sigma}{\mu}}\left(-\frac{\partial p}{\partial x}\right)\right]}\ ;\ J^* = \frac{J_z}{(y_0\sqrt{\sigma/\mu})\left(-\frac{\partial p}{\partial x}\right)} \end{aligned}\right\} \qquad \ldots (3)$$

All the physical variables are defined in Nomenclature.

4. The Energy Equation

Here we consider two cases :

(1) Two plates at different temperatures

(2) Temperature varying linearly along the plates.

Case (1) :

The energy equation for the fully developed flow is now given by

$$K\frac{d^2T}{dy^2} + \mu\left(\frac{du}{dy}\right)^2 + \frac{J_z^2}{\sigma} = 0 \qquad \ldots (4)$$

The boundary conditions are

$$T(y_0) = T_1 \quad \text{and} \quad T(-y_0) = T_2 \qquad \ldots (5)$$

In view of (3), equations (4) and (5) become

$$\frac{d^2\theta}{d\eta^2} + \left(\frac{du^*}{d\eta}\right)^2 + J^{*2} = 0 \qquad \ldots (6)$$

and

$$\theta(1) = \theta_1,\ \theta(-1) = \theta_2 \qquad \ldots (7)$$

where

$$\theta = \frac{K\mu T}{\left[y_0^2\left(-\frac{\partial p}{\partial x}\right)\right]^2} \qquad \ldots (8)$$

Substituting for u^* and J^* from (1) and (2) respectively, in (6), simplifying and integrating, the solution, satisfying (7), is given by

$$\theta = \frac{\theta_1+\theta_2}{2} + A_3(\eta^2-1) + A_4(\cosh 2M - \cosh 2M\eta)$$

$$+ A_5(\cosh M - \cosh M\eta) + \frac{\theta_1-\theta_2}{2}\eta \qquad \ldots (9)$$

where

$$A_1 = \frac{(I^*-1)M}{\sinh M}, \qquad A_2 = \frac{1+R^*+M\,V_0^*}{R^*\sinh M + M\cosh M},$$

$$A_3 = \frac{A_2^2-A_1^2-2}{4}, \qquad A_4 = \frac{A_1^2+A_2^2}{4M^2}, \qquad A_5 = \frac{2A_1}{M^2}$$

The temperature profiles are shown in figures 1 to 4 for different values of the parameters M, R^*, V_0^* and $T_1 = \left(\frac{\theta_1-\theta_2}{2}\right)$. Hughes & Young (1966)

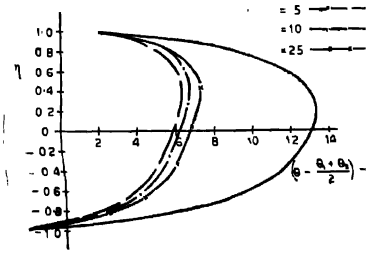

Figure 1. Temperature profiles ; $M=2$, $T_1=4$, $V_0^*=2$.

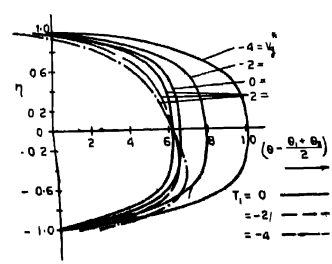

Figure 2. Temperature profiles ; $M=2$, $R^*=10$

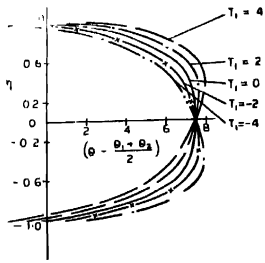

Figure 3. Temperature profiles ; (open circuit case) $M=2$.

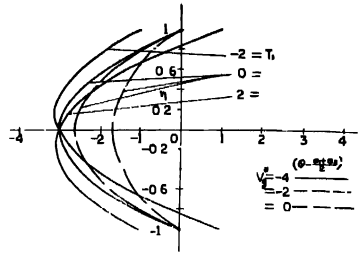

Figure 4 Temperature profiles ; $M=2$, $R^*=M/\tanh M$.

have described in short the interesting case of maximum power transfer between the external circuit and the flow device. The condition for this case as derived by them is that $R^* = \dfrac{M}{\tanh M}$.

The rate of heat transfer expressed in terms of the Nusselt number is given by (Hughes & Young 1966)

$$Nu = \frac{1}{\theta_1 - \theta_2} \left(\frac{d\theta}{d\eta}\right)_{\eta=-1} \tag{10}$$

From (9) and (10) we get,

$$Nu = \frac{M}{\theta_1 - \theta_2}\left[\, 2A_4 \sinh 2M + \frac{2(I^*-1)}{M}\,\right] - \frac{2A_3}{\theta_1 - \theta_2} + \frac{1}{2} \qquad \ldots (11)$$

The numerical values of Nu are entered in table 1. The bulk mean temperature is defined as

$$T_{im} = \frac{\int_{-1}^{1} u^*\theta \, d\eta}{\int_{-1}^{1} u^* \, d\eta} \qquad \ldots (12)$$

Substituting for u^* and θ from (3) and (9) respectively and simplifying, we obtain

$$T_{im} - \frac{\theta_1+\theta_2}{2} = \frac{4A_3\left(\dfrac{3-M^2}{3M^2}\cosh M - \dfrac{\sinh M}{M^3}\right) + \dfrac{2(I^*-1)}{M \sinh M}\left[\, 2\cosh^2 M - \dfrac{3\sinh 2M}{2M} + 1\,\right] + A_4\left(2\cosh 2M \cosh M + \dfrac{\sinh 2M \cosh M - 8\cosh 2M \sinh M}{3M}\right)}{\dfrac{2(1+R^*+MV_g^*)(M\cosh M - \sinh M)}{M^2(R^*\sinh M + M\cosh M)}}$$

$\ldots (13)$

Table 1- Values of Nusselt number(equation 11)

M	R^*	V^*_g \ T_1	−4	−2	2	4
2	5	−4	−15.4304	−31.3609	32.3609	16.4304
		−2	− 9.6416	−19.7832	20.7832	10.6416
		0	− 6.5056	−13.5112	14.5112	7.5056
		2	− 6.0225	−12.5449	13.5449	7.0225
		4	− 8.1922	−16.8843	17.8843	9.1922
	10	−4	−11.1074	−22.7149	23.7149	12.1074
		−2	− 8.6804	−17.8607	18.8607	9.6804
		0	− 7.1640	−14.8280	15.8280	8.1640
		2	− 6.5583	−13.6166	14.6166	7.5583
		4	− 6.8633	−14.2266	15.2266	7.8633
4	5	−4	−483	−966	967	484
		−2	−323	−647	648	324
		0	−214	−430	431	215
		2	−156	−313	314	157
		4	−148	−297	298	149
4	$R^* = \frac{M}{\tanh M}$	−4	9.3963	18.2925	−17.2925	− 8.3963
		−2	8.1488	15.7976	−14.7976	− 7 1488
		0	6 6514	12.8029	−11.8029	− 5.6515
		2	5.9043	9 3086	− 8.3086	− 3.9043
		4	2 9073	5.3147	− 4.3147	− 1.9073
2	$R^* \to \infty$ (open circuit case)		− 8.1517	−16.8033	17.8033	9.1517
4			−263	−528	284	264

The numerical value of $T_{im} - \frac{\theta_1+\theta_2}{2}$ are entered in table 2 for all cases.

Table 2. Values of $T_{im} - \frac{\theta_1+\theta_2}{2}$ (equation 13),

M	R^*/V_g^*	−4	−2	0	2	4
2	5	44	33	25	20	17
	10	36	31	26	23	20
4	5	343	250	183	141	124
	10	284	233	193	163	143
2	$M/\tanh M$	27.67	19.72	12.25	5.2716	−1.2324
4	$M/\tanh M$	75	61	47	34	21
	open circuit case	M			$T_{im} - \frac{\theta_1+\theta_2}{2}$	
		2			25	
		4			189	

Case 2 :

The temperature is now assumed to be varying linearly along the walls of the channel. This situation is then governed by the following energy equation

$$\rho C_p u \frac{\partial T}{\partial x} = K \frac{\partial^2 T}{\partial y^2} + \mu \left(\frac{\partial u}{\partial y}\right)^2 + \frac{J^2}{\sigma} \qquad \ldots (14)$$

The linear variation of temperature along the walls is represented by

$$T = Ax + G(y) \qquad \ldots (15)$$

Hence equation (14) in view of (15) and (3) reduces to the following non-dimensional form :

$$\frac{d^2G^*}{d\eta^2} + M^2\left\{\left(\frac{du^*}{d\eta}\right)^2 + J^{*2}\right\} - u^*S = 0 \qquad \ldots (16)$$

where

$$G^* = \frac{K\mu G}{\left[y_0^2\left(-\frac{\partial p}{\partial x}\right)\right]^2}, \quad Pr = \frac{\mu C_p}{K},$$

$$Re = \frac{\rho y_0}{\mu}\left[\frac{y_0^2}{\mu}\left(-\frac{\partial p}{\partial x}\right)\right], \; S_1 = \frac{K\mu y_0 A}{\left[y_0^2\left(-\frac{\partial p}{\partial x}\right)\right]^2}, \qquad \ldots (16a)$$

$$S = Pr\, Re\, S_1.$$

If the fluid and the walls are assumed to be at the same temperature, then the boundary conditions are

$$G^* = 0 \quad \text{at} \quad \eta = \pm 1 \qquad \ldots (17)$$

Hence the solution of (16), subject to the condition (17) is

$$G^* = \left\{\frac{A_2 S \cosh M}{M} - M^2 + \frac{M^2}{2}(A_2^2 - A_1^3)\right\}\left(\frac{\eta^2 - 1}{2}\right)$$

$$-\left(\frac{A_2 S}{M^3} + 2A_2\right)(\cosh M\eta - \cosh M)$$

$$-\frac{1}{8}(A_2^2 + A_1^2)(\cosh 2M\eta - \cosh 2M) \qquad \ldots (18)$$

The temperature profiles for G^* for different values of R^*, M, S, V_g^* are shown in figures 5 to 8.

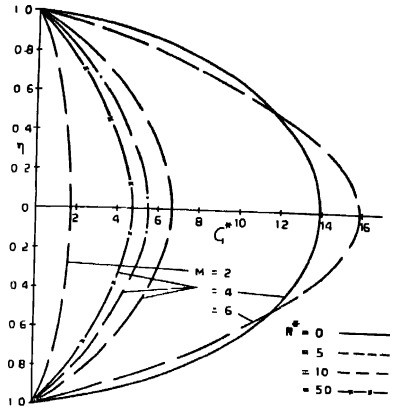

Figure 5. Temperature profiles, $S = 0.2$, $V_g^* = 4$

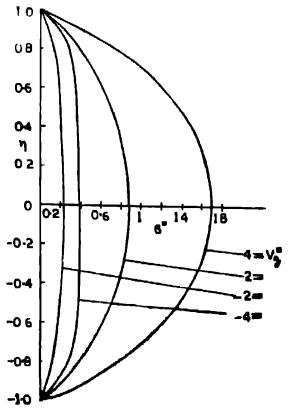

Figure 6. Temperature profiles, $M = 2$, $R^* = 5$, $S = 0.2$

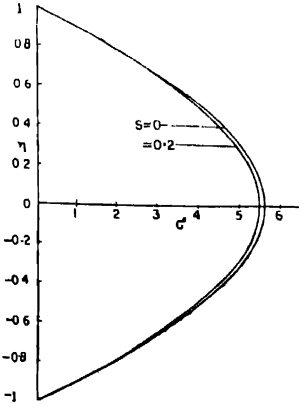

Figure 7. Temperature profiles, $M = 4$, $R^* = 10$, $V_g^* = 4$

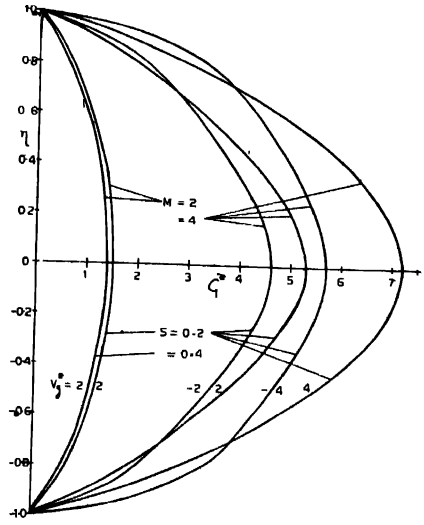

Figure 8. Temperature profiles, $R^* = M \tanh M$

The rate of heat transfer expressed in terms of the Nusselt number is defined as

$$Nu = \frac{y_0}{G_{y=0}} \left(\frac{dG}{dy} \right)_{y=-y_0} = \frac{1}{G^*_{\eta=0}} \left(\frac{dG^*}{d\eta} \right)_{\eta=-1} \qquad \ldots (19)$$

Hence from (18) and (19) we obtain,

$$Nu = \frac{\left[\left(\frac{A_2 S}{M^2} + 2A_1 M \right) \sinh M + \frac{1}{4}(A_1^2 + A_2^2) M \sinh 2M - \left\{ \frac{A_2 S \cosh M}{M} + \frac{M^2}{2}(A_1^2 - A_1^2 - 2) \right\} \right]}{\left[\left(\frac{A_2 S}{M^3} + 2A_1 \right)(\cosh M - 1) + \frac{1}{8}(A_1^2 + A_2^2)(\cosh 2M - 1) - \frac{1}{2} \left\{ \frac{A_2 S \cosh M}{M} + \frac{M^2}{2}(A_2^2 - A_1^2 - 2) \right\} \right]} \qquad \ldots (20)$$

The numerical values of Nu under different conditions are entered in table 3

Knowing u^* and J^* from (1) and (2) respectively, the mean temperature gradient A is found by considering the overall heat balance for a differential length of the channel as

$$A = \frac{\partial T}{\partial x} = \frac{\partial T_m}{\partial x} = \frac{q + \int_0^{y_0} \left[\mu \left(\frac{\partial u}{\partial y} \right)^2 + \frac{J_z^2}{\sigma} \right] dy}{y_0 v_a \rho C_p} \qquad \ldots (21)$$

where v_a is the average velocity and q is the heat flux at the plates. Hence by virtue of (3) and (16a), (21) reduces to the following non-dimensional form

$$S = Q + \int_0^1 \left[\frac{du}{d\eta} + J^{*2} \right] d\eta \qquad \ldots (22)$$

where

$$Q = \frac{q}{\left[\frac{y_0^3 \left(-\frac{\partial p}{\partial x} \right)^2}{\mu} \right]}$$

Substituting for u^* and J^* from (1) and (3) respectively, in (22) we obtain after simplification

$$S = Q + \frac{A_2^2 + A_1^2}{4M} \sinh M + \frac{A_1^2 - A_2^2}{2} - \frac{2A_1}{M} \sinh M + 1 \qquad \ldots (23)$$

From the practical point of view, it is important to know the variation of the difference between wall temperature and the mean temperature which is given by

$$T_w - T_m = Ax - \frac{1}{2y_0 v_a}\int_{-y_0}^{y_0} T(x,y)u(y)dy$$

$$= -\frac{1}{2y_0 v_a}\int_{-y_0}^{y_0} G(y)\,u(y)\,dy \qquad \ldots (24)$$

By virtue of (3) and (16a), (24) reduces to the following

$$(T_w - T_m)^* = -\tfrac{1}{2}\int_{-1}^{1} G^* u^* d\eta \qquad \ldots (25)$$

where

$$(T_w - T_m)^* = \frac{v_a}{\left[\frac{y_0^2}{\mu}\left(-\frac{\partial p}{\partial x}\right)\right]} \cdot \frac{K\mu(T_w - T_m)}{\left[y_0^2\left(-\frac{\partial p}{\partial x}\right)\right]^2}$$

Substituting for G^* and u^* from (18) and (1), respectively, in (25), carrying out the integration, we obtain

$$(T_w - T_m)^* = -\frac{1+R^*+MV_g^*}{M\sinh M(R+M\coth M)}\Big[\,2\left(B_1\frac{M^2+6}{2M^2}+D_2\right)\cosh M$$

$$-\frac{2}{M}\left(B_1\frac{M^2+2}{M^2}+D_2\right)\sinh M + B_2\frac{2M-\sinh 2M}{2M}$$

$$-\frac{B_3}{3M}(\cosh M\sinh 2M + 2\sinh M\cosh 2M)\Big] \qquad \ldots (26)$$

where

$$B_1 = \frac{1}{2}\left\{\frac{A_2 S\cosh M}{M} + \frac{M^2}{2}(A_2^2 - A_1^2 - 2)\right\},$$

$$B_2 = \frac{A_2 S}{M^3} + 2A_1 \quad ; \quad B_3 = \frac{A_1^2 + A_2^2}{8},$$

$$D_2 = \left(\frac{A_2 S}{M^3} + 2A_1\right)\cosh M + \frac{1}{8}(A_2^2 + A_1^2)\cosh 2M$$

$$-\frac{1}{2}\left\{\frac{A_2 S\cosh M}{M} - M^2 + \frac{M^2}{2}(A_2^2 - A_1^2)\right\}$$

$(T_w - T_m)^*$ is calculated from (26) in two different ways. The effects of M, R^*, V_g^* and S have been considered and they have been shown in figure 9–11 and

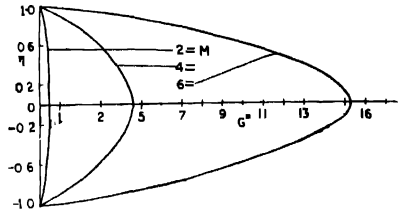

Figure 9. Temperature profiles, (open circuit case)

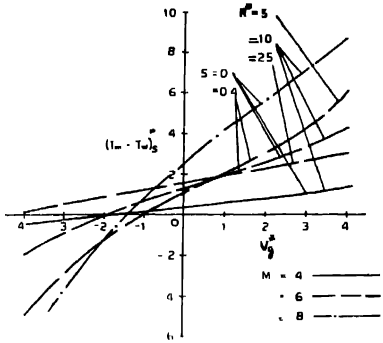

Figure 10. $(T_m - T_w)_S^*$ *vs* V_g^*; $M = 4$– $= 6$.

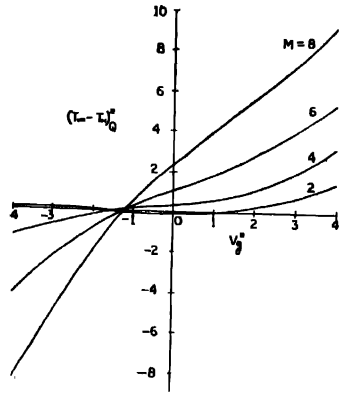

Figure 11. $(T_m - T_w)_S^*$ *vs* V_g^* ; $R^* = M/\tanh M$.

it is denoted by $(T_m - T_w)^*_S$. In figures 12–15 the effects of M, R^*, V_g^* and Q on $(T_w - T_m)^*$ have been shown and it is denoted now by $(T_m - T_w)^*_Q$. In this case the expression (23) for S is substituted in (25) and calculations are carried out for different values of Q.

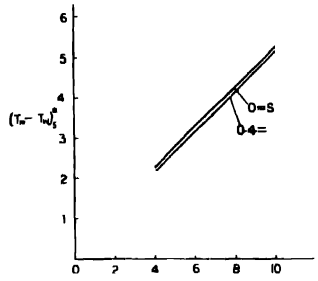

Figure 12. (open-circuit case) $(T_m - T_w)_S^*$ *vs* M,

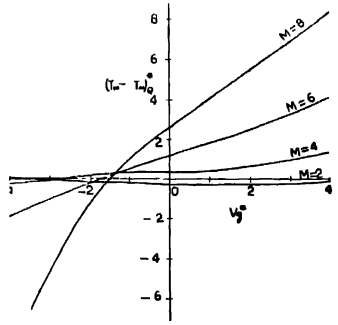

Figure 13. $(T_m - T_w)_Q^*$ *vs* V_g^* ; $R^* = 10$, $Q = 2$

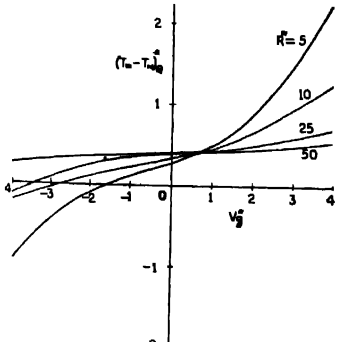

Figure 14. $(T_m - T_w)_Q^*$ *vs* V_g^*; $M = 4$, $Q = 4$

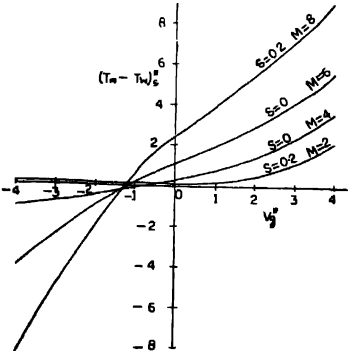

Figure 15. $(T_m - T_w)_Q^*$ *vs* V_g^* ; $Q = 2$, $R^* = M/\tanh M$.

3. Conclusions

Now the mhd channel flow described here is characterised as follows :

1. For $V_g^* = 0$ and $\partial p/\partial x$ negative, the fluid is flowing in the x-direction and hence the electric power is flowing into the external circuit provided $R^* \neq 0$ or $R^* \neq \infty$. Such a device is known as a mhd generator.

2 For $\partial p/\partial x$ negative, the fluid is pumped in the x-direction if $V_g^* > 0$ and hence the device is called an mhd accelerator. If $V_g^* < 0$, then the electromagnetic body force, due to V_g^*, opposes the flow in the positive x-direction and the flow in such a case is called a decelerated flow. In case of an mhd accelerator, R^* may be interpreted as the internal resistance of the power source.

3. $R^* \to \infty$ corresponds to an open circuit channel flow, whereas, for $R^* = 0$ and $V_g^* = 0$ corresponds to a short circuit case.

4. In case of an mhd generator, there is an interesting case of the maximum transfer of electrical power. The condition for this case, as derived by Hughes and Young (1966), is that $R^* = M/\tanh M$.

With these physical interpretations of the different parameters, in the problem, we have following conclusions in the two cases :

Case (1) :

In this case, the numerical values of the difference between the fluid temperature and the mean of the two wall temperatures is plotted under different conditions. Also in this case, T_1 is half the difference between the two wall temperatures and is positive when the temperature of the upper wall is greater than that of the lower wall and is negative the other way. In figure 1, the effects of the internal resistance in the case of an mhd accelerator on $\left(\theta - \frac{\theta_1+\theta_2}{2}\right)$ is shown. It is interesting to note here that $\left(\theta - \frac{\theta_1+\theta_2}{2}\right)$ is maximum when $R^* = 0$, *i.e.*, when the internal resistance of the power source is zero. But for $R^* > 0$, an increase in R^* leads to an increase in the value of $\left(\theta - \frac{\theta_1+\theta_2}{2}\right)$. In figure 2, the effects of V_g^* and T_1 on $\left(\theta - \frac{\theta_1+\theta_2}{2}\right)$ are shown. We conclude here that for constant T_1, the temperature is less in case of accelerated flow than that in decelerated flow. Moreover, as V_g^* decreases, $\left(\theta - \frac{\theta_1+\theta_2}{2}\right)$ increases. Regarding the effects of T_1, the temperature profiles are symmetrical when both the walls are at equal temperatures. But for T_1 negative, *i.e.*, when the temperature of the lower wall is greater than that of the upper wall, the symmetry is distorted and the temperature profiles are deflected towards the wall of higher temperature, which is so because the temperature of the fluid near the wall of higher temperature increases. Figure 4 gives the interesting result which is completely different from the earlier cases. It shows the behaviour of the fluid temperature when there is a maximum transfer of electrical power. In an mhd generator, or accelerator the value of $\left(\theta - \frac{\theta_1+\theta_2}{2}\right)$ is found to be negative for all

T_1, from which we can conclude that the temperature of the fluid, at this stage, is less than the mean temperature of the walls.

Case 2 :

In figure 5, the effects of M and R^* on the temperature profiles are shown. We observe that an increase in M leads to an increase in the G^*, when S, R^* and V_g^* are constant. However, in this case, an increase in R^*, the internal resistance of the power source, leads to a decrease in G^* when M, S and V_g^* are constant. From figure 6, we observe that temperature in case of an accelerated flow is greater than that in case of decelerated flow. From figure 7, we conclude that an increase in S leads to a decrease in G^* when M, R^* and V_g^* are constant. Figure 8 shows the temperature profiles when $R^* = M/\tanh M$. The effects of M, S and V_g^* are the same as before. In open-circuit case, an increase in M leads to an increase in G^*.

Figures 10 to 16 are particularly important from practical point of view for they show the variation of the difference between the mean temperature

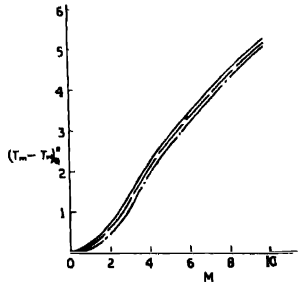

Figure 16. $(T_m - T_w)_Q^*$ *vs* M ; (open circuit case)

and the wall temperatures under different conditions. From figure 10, we conclude that $(T_m - T_w)^*_S$ increases with increasing V_g^* in case of an accelerated flow, whereas, it decreases with increasing V^*_g in case of a decelerated flow. An increase in M leads to an increase in $(T_m - T_w)^*_S$ when R^* and S are constant. But an increase in R^* leads to a decrease in $(T_m - T_w)^*_S$. An increase in S leads to a decrease in $(T_m - T_w)^*_S$. In figure 11, the values of $(T_m - T_w)^*_S$, in case of $R^* = M/\tanh M$ are plotted against V_g^*. $(T_m - T_w)^*_S$ behaves in the same manner as described above for figure 10. In open-circuit case also, the effects of M and S on $(T_m - T_w)^*_S$ are the same as those shown in figure 10.

In figures 13 to 16, the values of $(T_m - T_w)^*_Q$ are plotted. We observe here also that the effects of M, R^*, V_g^* are the same as described above in case of figures 10 to 12.

Case (1) :

1. From table 1 we conclude that (a) an increase in T_1 leads to a decrease in the value of the Nusselt number. But the rate of heat transfer is less when the temperature of the lower wall is greater than that of the upper wall; (b) Nu increases with increasing V_0^* or M; (c) in case of an mhd generator, R^* is the external resistance, whereas, R^* is the internal resistance of the power source in case of an mhd accelerator. Hence an increase in R^* leads to an increase in Nu when M, T_1 are constant.

2. From equation 13 and table 2 we conclude that the mean mixed temperature is not affected by the temperature difference of the plates. In case of an mhd generator the mean mixed temperature increases with increasing R^*. In accelerated flow, the mean mixed temperature increases with increasing R^*, the resistance of the internal power source, whereas, in decelerated flow, it decreases with increasing R^*. An increase in M always leads to an increase in the mean mixed temperature.

Case (2) (table 3) :

An increase in S, leads to an increase in the Nusselt number in case of an mhd generator and accelerator, whereas, in an mhd decelerating flow, an increase

Table 3. Values of Nusselt number (equation 20).

M	R^*	S/V_0^*	-4	-2	0	2	4
2	5	0	7.3315	5.6797	3.0841	2.7895	2.9659
		0.2	7 1920	5 8447	3 1859	2.8499	3.0169
		0 4	7.0592	6 0236	3.3031	2.9172	3.0721
	10	0	6.5502	4.6354	3 3809	2 9819	2.9422
		0 2	6.7158	4 8522	3.5133	3.0683	3.0106
		0.4	6.8931	5 1028	3.6673	3.1665	3 0866
4	5	0	6.4262	4.7272	3.2647	2.7116	2.9652
		0.2	6 4048	4 7239	3.2697	2.7182	2.9753
		0.4	6 3856	4.7207	3 2749	2.7249	2.9856
	10	0	5.4307	4.3581	3.4971	3.0131	2.9141
		0.2	5 4246	4.3609	3 5039	3.0211	2.9233
		0.4	5.4184	4.3637	3.5109	3.0293	2.9327
2	M/tanh M	0	6 2965	7 0330	2 6099	2.7540	3 1384
		0 2	6.1291	6 8926	2 6681	2.7968	3.1765
		0 4	5 9733	6.7593	2.7335	2.8429	3.2167
4		0	6.7425	4.8721	3.1862	2.6420	3.0473
		0.2	6.7159	4.8665	3 1907	2.6484	3.0581
		0.4	6.6896	4.8608	3.1953	2.6547	3.0691
	Open circuit case						
2		0	3.8053				
		0.2	3 9838				
		0.4	4.1922				
4		0	3.9373				
		0 2	3.9480				
		0.4	3.9588				

in S leads to a decrease in Nu when R^* is small and V_g^* is large, but for large R^*, Nu increases with increasing S. Nu also increases with increasing S in open-circuit case.

Acknowledgments

We are grateful to the referee whose comments lead to improvement of our paper.

References

Alpher R. A 1961 *Int J. Heat Mass Transfer*, **3**, 108

Hartmann J 1937 *Hg-Dynamics I, Danske Math-Phys Medd*, **15**, No 6.

Hartmann H & Lazarus F. 1937 *Hg-Dynamics II, Danske Math-Phys. Medd*, **15** No **7**.

Hughes W F. & Young F. J. 1966 *The Electromagnetodynamics of Fluids*, J. Wiley and Sons Inc.

Seigel, R. 1958 *J Appl. Mech.*, **25**, 415.

Soundalgekar V M. 1969 *Proc Nat Inst Sci India* **35A**, 329.

Sutton G. W. & Sherman A 1965 *Engineering Magnetohydrodynamics* (Mc-Graw Hill Co.).

Yen J. T. 1963 *Tr. ASME, J. Heat Transfer*, **85C**, No. **5**, 371.